Alexandria Engineering Journal (2017) xxx, xxx–xxx

HOSTED BY

Alexandria University

Alexandria Engineering Journal

www.elsevier.com/locate/aej
www.sciencedirect.com

ORIGINAL ARTICLE

Electromagnetic & thermal analysis of synchronous generator with different rotor structures for aircraft application

Deepak Arumugam [a,*], **Premalatha Logamani** [b], **Santha Karuppiah** [a]

[a] *Dept. of Electrical & Electronics Engineering, Sri Venkateswara College of Engineering, Chennai, India*
[b] *School of Electrical Engineering, VIT University, Chennai, India*

Received 23 January 2017; revised 22 February 2017; accepted 4 March 2017

KEYWORDS

Light combat aircraft;
High speed operation;
Salient pole & claw pole alternator;
Electromagnetic & thermal analysis

Abstract Alternator delivers power to a system which has high speed operations such as aircraft, marine industry, and automobile industries. So, it is necessary to evaluate the performance of this alternator during high speed operations. Finite Element Analysis (FEA) is an effective tool to analyze the performance of electrical machines with certain boundary conditions. In this paper, the FEA analysis of the 5 KW alternator with two different rotor structures for high speed operation is presented. The transient electromagnetic FEA has been carried out which forms the basis for thermal modeling and thermal analysis of the alternator. Finally the overall electromagnetic and thermal performance of a prototype alternator with different rotors is compared experimentally.

1. Introduction

Alternator supplies power to the emergency loads present in the modern aircraft vehicles. Generally the voltage required for these vehicles ranges from 24 V to 240 V. Also, the speed of these vehicles varies from 7000 rpm to 24,000 rpm [1,8,9]. Even though these vehicles require DC power, this power is obtained from alternator through diode bridge rectifier, because this system has more efficiency and better performance [14]. In general alternator has two main parts. Armature (stator) acts as the stationary part and the field (rotor) acts as the rotating part. Mainly two types of alternators are used. They are salient pole alternator and cylindrical pole alternator. Generally salient pole type generator is used for low and medium speed applications and it has large diameter, short axial length with a large number of projecting poles. On the other hand, cylindrical pole synchronous generator is used for high speed applications with large axial length and small diameter with circular coil. The major requirement of the synchronous generator for high speed applications is high power density, compact design, less components, ability to withstand high temperature, and high reliability with high efficiency [11]. The power density of the machines is measured by the amount of mechanical power produced per unit volume. The compact design value can be obtained by using different iterations conducted during the design process.

If the thermal conductivity of the winding is increased, then the cooling of the generator can be increased and additional power is produced [18]. The modern computer based design

* Corresponding author.
E-mail address: adeepakceg@gmail.com (D. Arumugam).
Peer review under responsibility of Faculty of Engineering, Alexandria University.

http://dx.doi.org/10.1016/j.aej.2017.03.020

packages are used to perform the thermal analysis of electrical machines along with electromagnetic analysis. The major advantage of these packages is to optimize the thermal performance in terms of design, cost, weight, losses and efficiency [3]. The core material and insulation selection also play a vital role in thermal analysis. The design flow diagram for modern electrical motors is given in [7]. In electrical machines thermal analysis can be conducted by two different approaches. They are analytical and numerical analyses. In analytical method the losses that occur in the machines, efficiency and temperature can be calculated. Here heat rate and flow rate are obtained by calculating conduction, convection, radiation resistances and machine losses such as core loss, copper loss and mechanical losses. This analysis provides efficient and fast result but it cannot provide heat flow path and point out where the maximum heat is produced in the machines. On the other hand, numerical analyses consume large time for simplification but give heat flow rate very accurately for any complex regions [21–23,25]. Computational Fluid Dynamics (CFD) and Finite Element Analysis (FEA) are the two major classifications of numerical analysis. In general CFD is suitable for analyzing liquid or flow system and FEA is suitable for solid structure. FEA is the best method to conduct electromagnetic and thermal analyses of electrical machines. The history, different types of software tools, steps required for design, and advantages and disadvantages of FEA are given in [6]. The coupled electromagnetic and thermal analysis using multi-physics software requires large computing time and also it gives less accurate result. The electromagnetic and thermal interaction of claw pole alternator using multi-physics software has been discussed in [20]. The combined lumped element and finite element method is used for reliable power conversion calculations with simple equivalent circuit model. Based on these methods analysis of permanent magnet synchronous generator at a speed of 15,000 rpm with 8 MW power rating has been carried out for gas turbine applications in [5]. The FEA 3D analysis of inter polar claw pole alternator with 42 V, 8 kW rating and 14 V, 5 kW rating has been given in [17]. The modeling of various electrical machines with combined electromagnetic and thermal analysis has been presented for various applications in [10,26,19,16,24,15,13].

The above literature, however, does not deal with the combined electromagnetic and thermal analysis of alternator pertaining to a specific dimension, high speed and high power rating. Hence this work proposes the FEA analysis of alternator with different rotor structures with constrained dimensions for aircraft applications. The simulation analysis and prototype model of 5 KW alternator with salient and non-salient poles are presented. The organization of the paper is as follows: Section 2 deals with the description of aircraft power system structure. Thermal modeling of alternator with different rotor structures is given in Section 3. The simulation results of the alternator for various rotor topologies are given in Section 4. The experimental results are presented in Section 5. The work is concluded in Section 6.

2. Description of aircraft power system

The Indian aircraft project is now called the Light Combat Aircraft (LCA) in order to create an identity distinct from the Light Weight Fighter concept. In the early 1980s, India, knowing well that the Mig-21s, Mig-23s, and a variety of other aging Russian fighters composing a vast percentage of their air power would soon grow obsolete, decided to produce a new fighter to replace the MiG-21 "Fishbeds" legacy. The new aircraft would be of indigenous design, and its development would fall under the care of India's own Aeronautics Limited. The aircraft that would spawn from the program was designated the Light Combat Aircraft and it would be one of the world's lightest, yet most capable dedicated multi-role aircraft of all times [12]. In LCA, 30–60 KVA generator provides electrical power supply to all electrical loads. When this power system fails, the backup power supply supports and is called integrated generator system (IGS) providing power supply to emergency loads such as cabin lighting, food preparation, gunshot and cockpit. This IGS consists of 3 electrical generators, namely permanent magnet synchronous generator, Brushless synchronous generator (also called Main exciter) and Synchronous generator (also called main generator) being mounted on single shaft which is driven by aircraft engine gear box. The basic structure of IGS is shown in Fig. 1. Moreover, the space constraint in an aircraft proscribes the IGS to be housed with any external cooling arrangements. The maximum diameter of the all three generators is limited up to 140 mm. Also aircraft engine rotating speed lies between 7000 rpm and 24,000 rpm [2]. So, it does not provide any external cooling arrangements at this dimension for high speed operations. Due to these reasons, much heat is produced in the main generator. So it is necessary to perform electromagnetic and thermal analysis of the above generators to measure the performance of each generator for high speed operations.

Synchronous generator armature is the stationary part and field is the rotating part of the machine. Normally two types of synchronous generators are used. They are salient pole synchronous generator and cylindrical pole synchronous generator. Generally salient pole type is used for low and medium speed applications and cylindrical pole synchronous generator is used for high speed applications. The analytical design of the generator is carried out using the following expressions.

3. Analytical design equations of synchronous generator

The analytical design equations & values of the salient pole and claw pole alternator are presented in the following sections.

3.1. Analytical design of salient pole alternator

The rms value of generated emf equation of the synchronous generator is

$$E_{ph} = 4K_f K_d K_c T f \phi \text{ in volts} \quad (1)$$

When the machine electrical equations are transformed from abc to dq reference frame model, the following equations are obtained.

In armature section voltage equation is

$$V_d = \frac{d\lambda_d}{dt} - \lambda_q \omega - R_a i_d \quad (2)$$

$$V_q = \frac{d\lambda_q}{dt} + \lambda_d \omega - R_a i_q \quad (3)$$

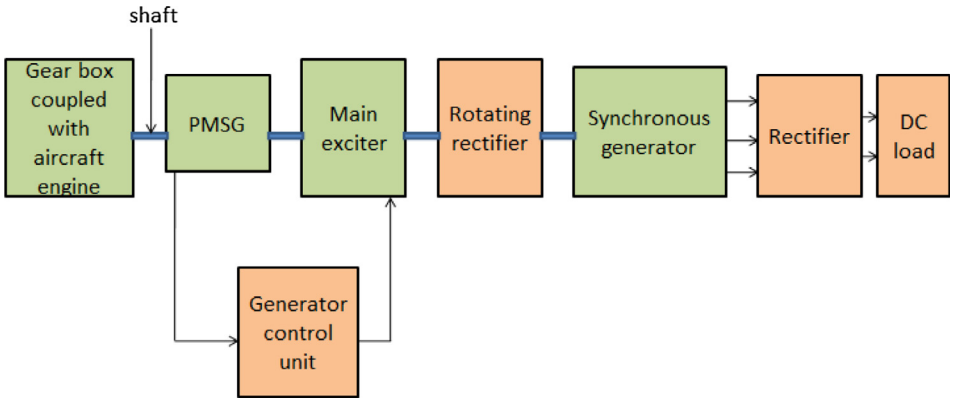

Figure 1 Basic structure of IGS system.

In field section voltage equation is

$$e_{fd} = \frac{d\lambda_{fd}}{dt} + R_{fd} i_{fd} \tag{4}$$

$$0 = \frac{d\lambda_{1d}}{dt} + R_{1d} i_{1d} \tag{5}$$

$$0 = \frac{d\lambda_{1q}}{dt} + R_{1q} i_{1q} \tag{6}$$

In armature section flux linkage equation is

$$\lambda_d = -(L_{ad} + L_l) i_d + L_{ad} i_{fd} + L_{ad} i_{1d} \tag{7}$$

$$\lambda_q = -(L_{aq} + L_l) i_q + L_{aq} i_{1q} \tag{8}$$

In field section flux linkage equation is

$$\lambda_{fd} = (L_{ad} + L_{fd}) i_{fd} - L_{ad} i_d + L_{ad} i_{1d} \tag{9}$$

$$\lambda_{1d} = (L_{ad} + L_{1d}) i_{1d} - L_{ad} i_d + L_{ad} i_{fd} \tag{10}$$

$$\lambda_{1q} = (L_{aq} + L_{1q}) i_{1q} - L_{aq} i_q \tag{11}$$

$$\text{KVA output } Q = 1.11 B_{av} A C k_w 10^{-3} v_a^2 (L/n_s) \tag{12}$$

$$\text{Turns per phase } T_{ph} = \frac{E_{ph}}{4.44 \Phi f K_w} \tag{13}$$

$$\text{Current in each conductor } I_z = \frac{\text{KVA} * 10^3}{3 E_{ph}} \tag{14}$$

$$\text{Minimum width of the tooth } W_{t(min)} = \frac{\Phi}{1.8 (S/p) \Psi L_i} \tag{15}$$

$$\text{Stator Mean Diameter (MD)} = (\text{Slot root dia} + \text{Slot tip dia})/2 \tag{16}$$

$$\text{Pole Mean Diameter (PMD)} = (\text{Pole Tip Dia} + \text{Pole Root Dia})/2 \tag{17}$$

$$\text{Self inductance } L_g = \frac{\mu_0 \prod L_{stk} r_1 T_p^2}{2 P_p^2 g'} \tag{18}$$

$$\text{The stator DC resistance per phase } r_{dc} = \rho T_{ph} \frac{L_{mts}}{a_s} \tag{19}$$

$$\text{Armature mmf per pole ATa} = 2.7 \frac{I_{ph} T_{ph} K_w}{p} \tag{20}$$

$$\text{Resistance of the field winding } r_f = \frac{T_f \rho L_{mtf}}{a_f} \tag{21}$$

The theoretical design values are listed in Table 1 which are used to create the model of the generator in simulation software.

3.2. Analytical design equations of CPA

Based on the salient pole parameter input, stator design is carried out using theoretical design equations and few of them are presented below. The design of claw pole rotor is carried out based on the theoretical equations and it is verified using design software RMxprt. The design can be optimized by using MATLAB program and more iteration with Newton Raphson algorithm. The major factor considered for getting optimized design is efficiency, Temperature, different load conditions (100%, 125% and 150% of full load) and losses. The optimized design value can be achieved only at 59th iterations and it is listed in the design table. The general design expressions are given below.

KVA rating of a 3 phase synchronous machine is

$$\text{KVA} = 1.1 K_{w1} B_{avg} q D^2 L n_s * 10^{-3} \tag{22}$$

where K_{w1} is the winding factor for stator winding, B_{avg} the specific magnetic loading, q the specific electric loading, D the diameter of stator bore and n_s the synchronous speed in rps.

RMS value of the fundamental induced EMF per phase of claw pole machine is

$$E_1 = 4.44 K_{w1} \Phi_1 n P I_f \text{ in volts} \tag{23}$$

where Φ_m is the fundamental flux passing through the core, n the speed in rps and I_f the field current in amps.

$$\text{Stator Mean Diameter (MD)} = (\text{Slot root dia} + \text{Slot tip dia})/2 \tag{24}$$

$$\text{Pole Mean Diameter (PMD)} = (\text{Pole Tip Dia} + \text{Pole Root Dia})/2 \tag{25}$$

Table 1 Analytical design data of salient pole alternator.

Parameters	Specification	Analytical output	RMxprt output
Rated power in W	P	5000	5000
Rated DC voltage in V	V_{dc}	28	28
Rated current in A	I	180	178.8
Stator outer diameter in mm	D_{os}	140	139.5
Rotor outer diameter in mm	D_{or}	91.86	91
Length of the airgap in mm	L_g	0.37	0.37
Speed in rpm	N	9000	9000
Slot type	–	Trapezoidal	Trapezoidal
Number of slots	S	24	24
Number of poles	p	4	4
Pole arc/pole pitch	τ	0.78	0.7
Stacking factor	K_s	0.95	0.95
Power factor	$\cos\varphi$	0.88	0.88
Frequency in Hz	f	292	292
Flux density in mWb/m^2	B	2.7	2.72
Flux/pole k_{Max}	Φ	107.2	107
Stator copper loss in W	$P_{cu\ stator}$	346.2	360
Rotor copper loss in W	$P_{cu\ rotor}$	162	161.26
Stator core loss in W	$P_{iron\ stator}$	50.7	51.23
Friction & windage loss in W	P_{fw}	200	200
Total losses in W	P_{total}	758.9	772.59
Efficiency in %	η	86.82	86.66

$$\text{Self-inductance } L_g = \frac{\mu_0 \prod L_{stk} r_1 T_p^2}{2P_p^2 g'} \tag{26}$$

where g' is the gap coefficient $= C_g\, g$ and p = number of rotor poles.

$$\text{Peripheral speed} = \pi d n_s \frac{m}{S} \tag{27}$$

where d = rotor diameter in mm.

The shape of the pole is determined by the pole pitch and it is denoted by τ,

$$\tau = \frac{\pi d m}{p} \tag{28}$$

$$\text{Flux per pole } \Phi_p = \frac{2 l_{stack} T_{ph} B_{av}}{\pi} \tag{29}$$

$$\text{Airgap magnetic reluctance } R_g = \frac{1}{\mu_0} \frac{g K_c}{\alpha_p \tau l_{stack}} \tag{30}$$

where K_c is Carters coefficient.

The losses occurring in claw pole machine are stator iron losses, stator copper losses, rotor copper losses, rotor claw harmonic losses, mechanical losses and diode rectifier losses (if diodes presented internally in CPA). The copper loss expressions of the claw pole alternator are

$$\text{Stator copper loss } P_{cus} = 3R_1 I_1^2 \tag{31}$$

$$\text{Rotor copper loss } P_{cur} = R_f I_{faverage}^2 \tag{32}$$

The power factor of the CPA is $\cos\varphi$

$$= \sqrt{1 - \left[\frac{\omega L_e I_1}{V_1}\right]^2} \tag{33}$$

where V_1 and I_1 are the fundamental voltage and current, L_e is the average sub transient inductance and ω is the angular frequency. The accuracy of the analytical design values can be checked into the RMxprt software. The comparison between analytical design values and RMxprt software output values is given in Table 2.

4. Electromagnetic analysis

4.1. Analytical design

The simulation analysis of the alternator was carried out using FEA software's MagNet and ThermNet. MagNet software is used to evaluate electromagnetic analysis and ThermNet is

Table 2 Analytical design of CPA.

Parameter	Specification	Analytical value	RMxprt output
Rated power in W	P	5000	5000
Rated DC voltage in V	V_{dc}	28	28
Rated current in A	I	180	178.8
Stator outer diameter in mm	D_{os}	140	139.5
Rotor outer diameter in mm	D_{or}	91.86	91
Length of the airgap in mm	L_g	0.37	0.37
Speed in rpm	N	9000	9000
Number of slots	S	24	24
Number of poles	p	4	4
Stacking factor	K_s	0.95	0.95
Winding factor	K_w	0.966	0.965
Power factor	$\cos\varphi$	0.88	0.88
Frequency in Hz	f	292	292
Field excitation current in A	I_f	10	10
Flux density in mWb/m^2	B	3.3	3.28
Flux/pole in k_{Max}	Φ	107.2	107
Number of turns in rotor coil/pole	T_{rph}	160	160
Conductors used in stator in SWG	–	18 * 4 & 19 * 1	18 * 4 & 19 * 1
Conductors used in rotor in SWG	–	19 * 1	19 * 1
Pole height in mm	h_p	23	23
Width of the pole in mm	W_p	6.3	6.9
Number of parallel paths	A	2	2
Stator copper loss in W	P_{cus}	346.2	360
Rotor copper loss in W	P_{cur}	124	119.23
Stator core loss in W	P_{irons}	50.7	51.23
Friction & windage loss in W	P_{fw}	186	178.5
Total losses in W	P_{total}	706.9	708.96
Efficiency in %	η	87.61	87.58

Please cite this article in press as: D. Arumugam et al., Electromagnetic & thermal analysis of synchronous generator with different rotor structures for aircraft application, Alexandria Eng. J. (2017), http://dx.doi.org/10.1016/j.aej.2017.03.020

used to find thermal performance of electrical machines. In this analysis two different rotor structures are to be considered. They are salient pole rotor and claw pole rotor. In salient pole rotor rectangular type coil is used and circular type of coil is used in claw pole rotor. The simulation model of salient pole and claw pole structure is shown in Fig. 2.

4.2. Electromagnetic field analysis of SPA

The 2D electromagnetic analysis of salient pole generator was carried out using MagNet software version 7. It was used to find flux density plot, voltage and current. In this simulation analysis, a 5 KW/28 V, 24 stator slot, 4 field pole salient pole alternator were taken for analysis at a speed of 9000 rpm. In the simulation circuit, the size of the mesh was 2 mm, the total number of nodes was 17,966, the number of edges was 78,965, and the number of faces was 36,489. The overall structure of the salient pole alternator obtained from simulation is shown in Fig. 3. The stator and the rotor cores were made with hyperco material and the winding was designed with copper material.

The total steps fixed to solve the problem were 10. The problem was solved with 2D transient with motion condition and total time required to solve the problem was 6 h 33 min. The flux linkage plot is shown in Fig. 4 and it is observed that the flux distribution is uniform in the generator. The maximum value of flux density is 2.733 mWb/m^2. The voltage induced in the armature winding was 27.5 V and the current flowing through the armature winding was 176 A. Both voltage and current waveform settled its peak value in each phase. It is shown in Fig. 5.

4.3. Electromagnetic field analysis of CPA

In this section the simulation analysis of 5 KW/28 V, 4 pole and 24 slot claw pole alternator with concentrated stator winding and cylindrical rotor winding is presented. In claw pole alternator field is distributed in all the 3 axes. So it is necessary to simulate claw pole alternator using 3D analysis. The problem formulation is based on vector potential with magneto dynamic computations. The size of each individual mesh was 2 mm, the number of nodes was 57,317, the number of edges was 178,965, and the number of faces was 121,727. The overall simulation model of CPA is shown in Fig. 6.

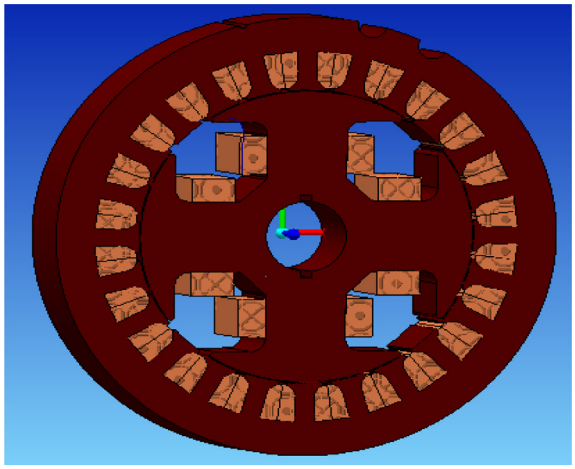

Figure 3 Simulation model of SPA.

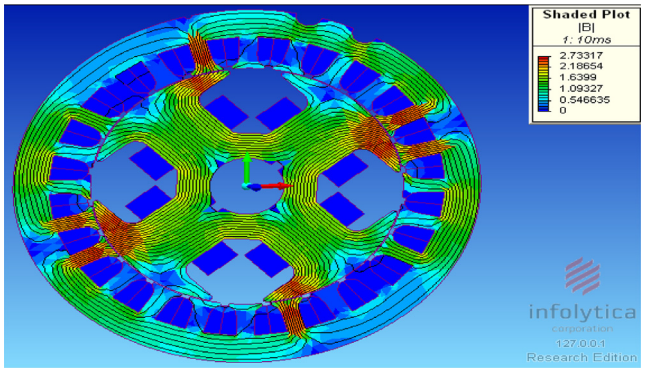

Figure 4 Flux density plot of SPA.

The total steps fixed to solve the problem were 10 and the total time taken to solve the problem was 32 h and 12 min. The stator and the rotor cores were made with hyperco material and the winding was designed with copper material. The flux density plot of a CPA is shown in Fig. 7. The maximum value of flux density obtained from the simulation was 3.28 mWb/m^2. From Fig. 8, voltage in the armature winding is 28 V and the current through the armature winding is 180 A.

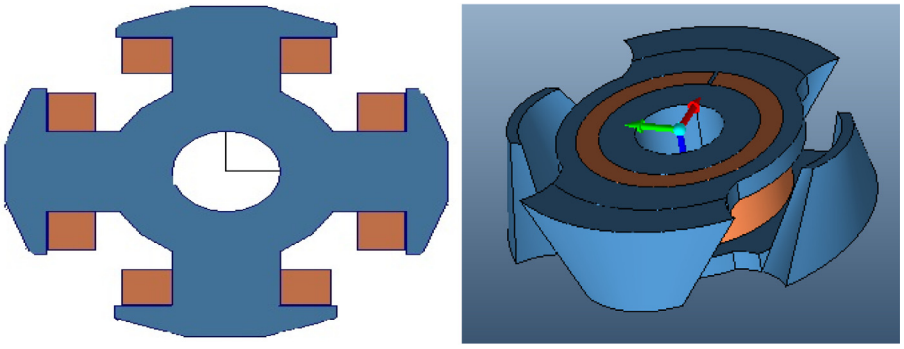

(a) Salient pole rotor (b) Claw pole rotor

Figure 2 Basic structure of salient pole and claw pole rotor.

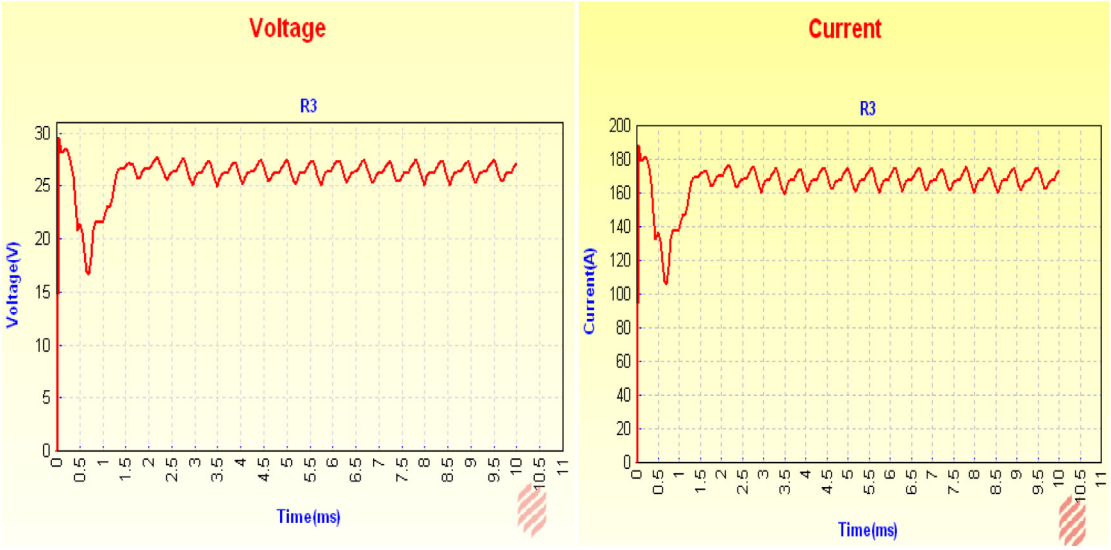

Figure 5 Load voltage and current in SPA.

From the above electromagnetic field analysis, it is clear that both salient pole and claw pole produce the same output for the same dimensions, the number of slots, and the number of poles. But the flux density value is slightly higher in the claw pole alternator than in the salient pole alternator.

5. Thermal analysis

In this section the thermal modeling and thermal analysis of the alternator with different rotor structures are presented.

5.1. Thermal modeling of the synchronous generator

Analytical method is more accurate and gives very fast result. In analytical method, it is necessary to find the thermal equivalent model of the alternator. The thermal modeling of alternator is given in [2,4]. The general expressions used in the thermal modeling of alternator are given below.

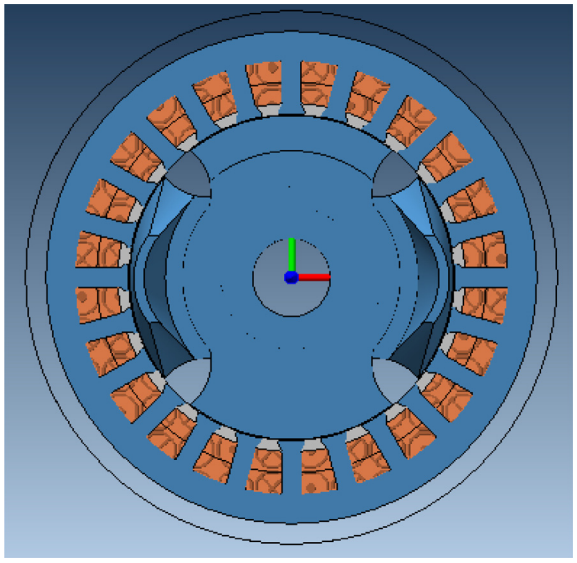

Figure 6 Simulation model of CPA.

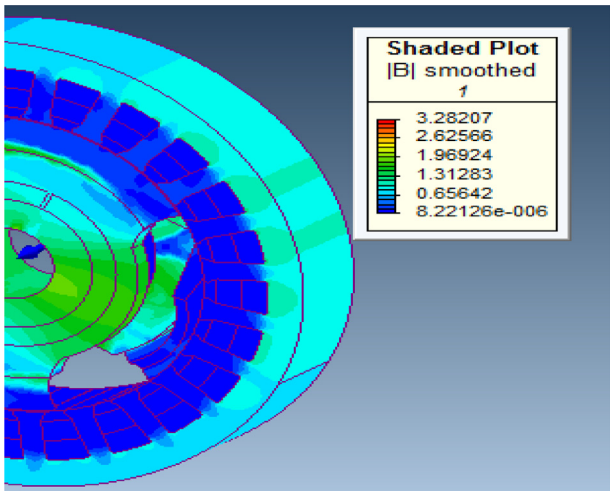

Figure 7 Flux density plot of CPA.

The conduction thermal resistance is given by

$$R_{conduction} = \frac{L}{kA} \tag{34}$$

where L is the path length in meters, A the path area in square meters and K is the thermal conductivity of the material in °C.

The convection thermal resistance of the surface is

$$R_{convection} = \frac{1}{Ah_R} \tag{35}$$

where A is the surface area in square meters.

h_R is heat transfer coefficient in watt per square meter per °C and it is given by

$$h_R = \sigma \varepsilon F_{1-2} \frac{(T_1^4 - T_2^4)}{(T_1 - T_2)} \tag{36}$$

where $\sigma = 5.669 \times 10^{-8}$ W/(m^2 K^4), ε is emissivity of the surface, $F_{1\text{-}2}$ is view factor for dissipating surface 1 to the absorbing surface 2 and T_1, T_2 are temperatures of surfaces 1 and 2.

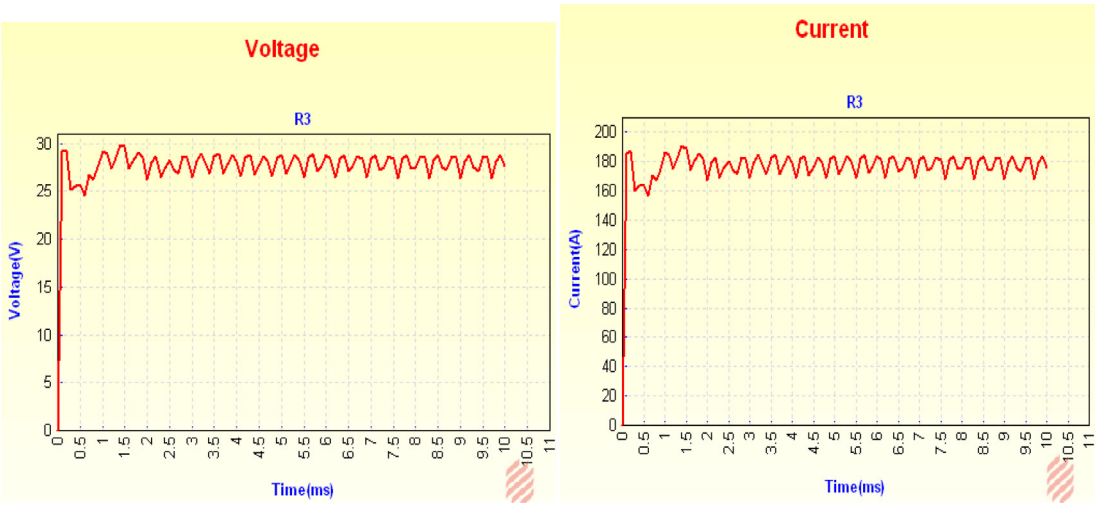

Figure 8 Voltage and current at the load.

The radiation thermal heat resistance for a given surface is given by

$$R_{radiation} = \frac{1}{Ah_C} \tag{37}$$

where h_C is the convection heat transfer coefficient in watt per square meter °C.

The total heat flow rate in the given surface is

$$\text{Heat flow} = \frac{\Delta T}{R} \tag{38}$$

where ΔT is the surface temperature rise and R is the flow resistance.

The surface temperature rise ΔT is given by

$$\Delta T = \frac{\text{Power dissipated in watts}}{\text{Volume flow rate} * \text{Density} * C_p} \tag{39}$$

where C_p is the specific heat capacity in J/kg/°C.

Thermal capacitance (C) is the important factor in thermal network used to mention the heat source at each node. It is given by

$$C = \rho V C_p \tag{40}$$

where ρ is the density in kg/m^3 and V is the volume in m^3.

The above expressions are used to find heat flow rate of the alternator. But it is necessary to define losses associated with the alternator, because losses are also an important factor for generating heat in electrical machines. In general, the major losses produced in the alternator are iron loss, copper loss, mechanical loss, and stray losses. The general expressions for the above mentioned losses are given below based on axial length and end windings.

The iron loss is defined as

$$\text{Rotor Iron Loss} = \frac{\text{Total iron loss} * 0.15}{\text{Number of rotor poles}} * \frac{1}{\text{Number of axial planes} * \text{Number of plane nodes}} \tag{41}$$

$$\text{Stator Copper Loss} = \frac{\text{Total iron loss} * 0.85}{\text{Number of stators lots}} * \frac{1}{\text{Number of axial planes} * \text{Number of plane nodes}} \tag{42}$$

In general copper loss is defined as

$$P_{\text{Cu}} = I^2 R \tag{43}$$

Copper loss based on axial length and end windings is

$$\text{Rotor Copper Loss}_{\text{Length}} = \frac{\text{Total copper loss}}{\text{Number of rotor poles}} * \frac{\text{Axial length of the segment}}{\text{Total length of coil around pole}} \tag{44}$$

$$\text{Rotor Copper Loss}_{\text{end winding}} = \frac{\text{Total copper loss}}{\text{Number of rotor poles}} * \frac{\text{Coil end turn length}}{\text{Total length of coil around pole}} \tag{45}$$

$$\text{Stator Copper Loss}_{\text{Length}} = \frac{\text{Total copper loss}}{\text{Number of stators lots}} * \frac{\text{Axial length of the segment}}{\text{Total core length}} \tag{46}$$

$$\text{Stator Copper Loss}_{\text{end winding}} = \frac{\text{Total copper loss}}{\text{Number of stator slots}} * \frac{\text{Coil end turn length}}{\text{Total core length}} \tag{47}$$

Total stray losses are given by

$$P_{stray} = \text{Load fraction}^{0.8} * \left(\text{Machine rating} * \left(\frac{50}{f}\right)\right)^{0.59} * \left(\frac{f}{50}\right)^{1.5} \tag{48}$$

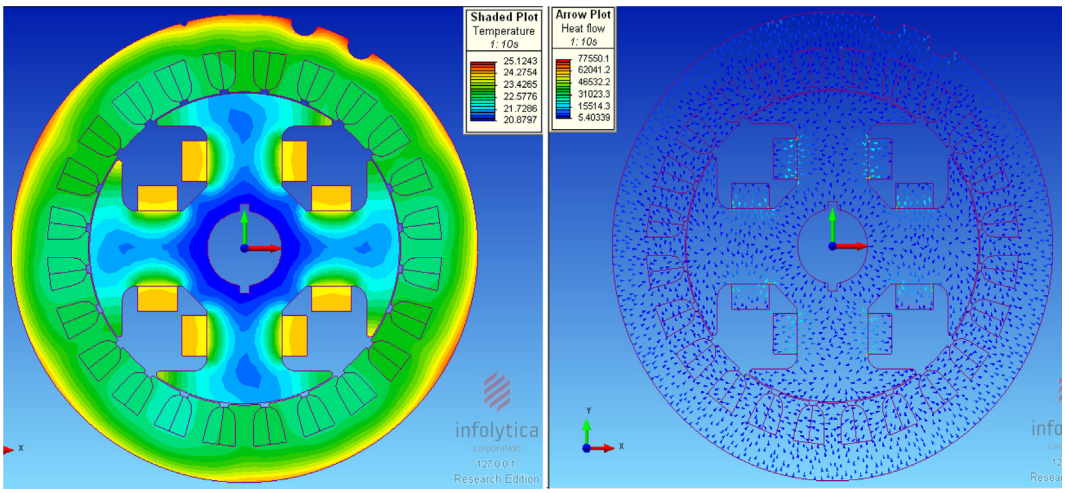

Figure 9 Temperature and heat flow plot of SPA at 9000 rpm.

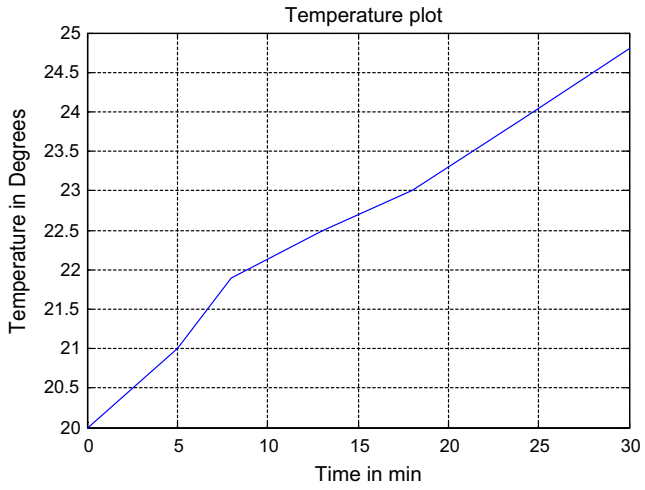

Figure 10 Temperature during transient condition in SPA.

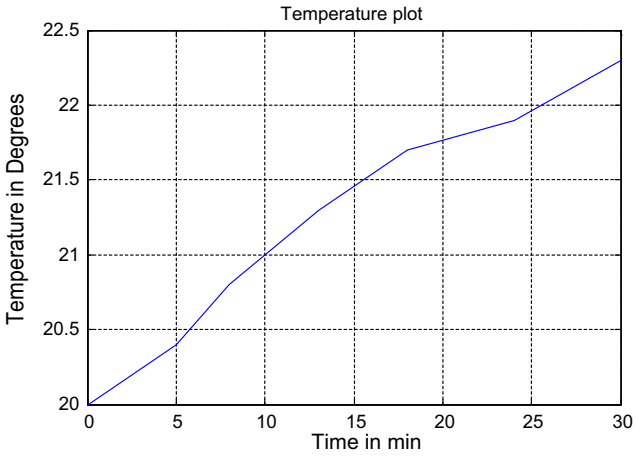

Figure 12 Temperature during transient condition in CPA

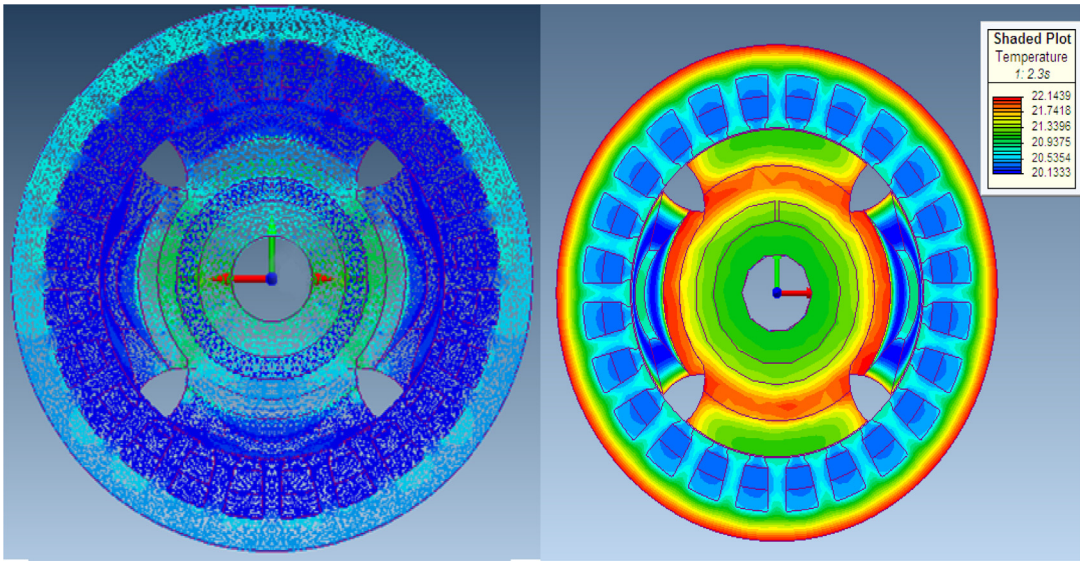

Figure 11 Temperature and heat flow of CPA at 9000 rpm.

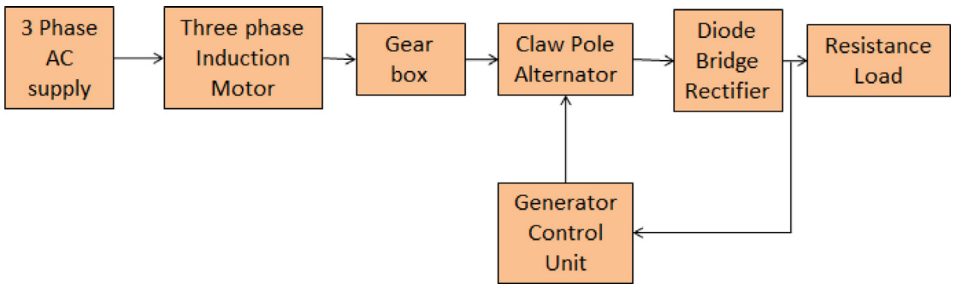

Figure 13 General experimental setup.

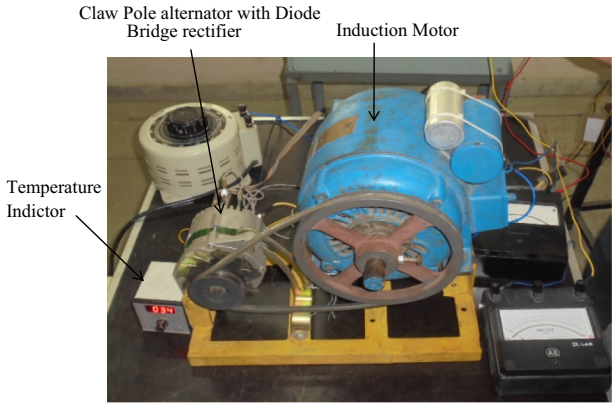

Figure 14 Prototype model of 5 KW salient pole alternator.

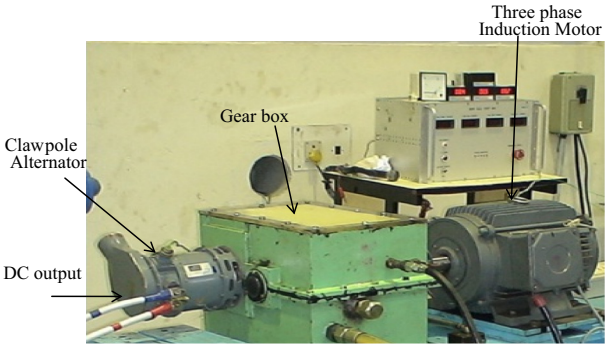

Figure 15 Prototype model of the 5 KW claw pole alternator.

Based on the above expressions the total losses, losses in rotor and stator and thermal resistances can be obtained analytically.

5.2. Thermal analysis of SPA

Generally thermal analysis of the machine helps to find total temperature produced in the machine and heat flow direction in the machine. In coupled magnetic field and thermal analysis, the result of electromagnetic field analysis (i.e., losses) forms the input for thermal analysis. The MagNet and ThermNet are tightly integrated which facilitates the results from MagNet to be readily adapted in ThermNet for thermal analysis.

The boundary condition for this problem is convective heat transfer coefficient 75 W/m^2 °C, emissivity 0.999 and surrounded by thermal environment with a temperature of 120 °C. This solver takes 28.7 min to solve this problem. After solving the problem, the temperature distribution in the generator is shown in Fig. 9 and the maximum temperature produced in the generator was 25.12 °C. From the figure it is concluded that the maximum temperature generated at the stator core and rotor conductors. Also the heat flow plot is shown in Fig. 9. During transient period the temperature keeps on increasing and reaches nearly 25 °C when the machine runs at 9000 rpm with full load condition. Temperature plot during transient condition is shown in Fig. 10.

5.3. Thermal analysis of CPA

The thermal analysis of the claw pole alternator was carried out using ThermNet software. This generator construction and design values are the same as those of MagNet software design. Additionally it has three boundary conditions. The boundary condition assumed in this generator is convective heat transfer coefficient is 75 W/m^2 °C and heat surrounded in the generator is 120 °C.

The temperature developed in the generator and heat flow plot is shown in Fig. 11. In this figure the maximum temperature concentrated at rotor conductors and stator core. It is also observed from the figure that the maximum heat produced in the generator is 22.14 °C. Similarly during transient period the temperature value slightly increases at full load condition and this value approximately equals to 22.3 °C. It is shown in Fig. 12.

From the above thermal analysis using simulation software it is noticed that the maximum heat generated at rotor coil and stator core outer surface for both the cases. Similarly the heat generated in claw pole rotor is less than salient pole rotor, because claw pole rotor has large airgap and airflow.

6. Experimental validation

The general structure of the experimental setup for the alternator with different rotor is shown in Fig. 13. In this figure the generator control unit is the combination of rectifier and Cuk converter to provide constant DC current to the field windings of both the alternators. Diode bridge rectifier circuit is connected inside the alternator.

The prototype model of a 5 KW SPA with 24 slots and 4 poles is shown in Fig. 14. In this figure both single phase induction motor and SPA are coupled with pulley having a speed

Please cite this article in press as: D. Arumugam et al., Electromagnetic & thermal analysis of synchronous generator with different rotor structures for aircraft application, Alexandria Eng. J. (2017), http://dx.doi.org/10.1016/j.aej.2017.03.020

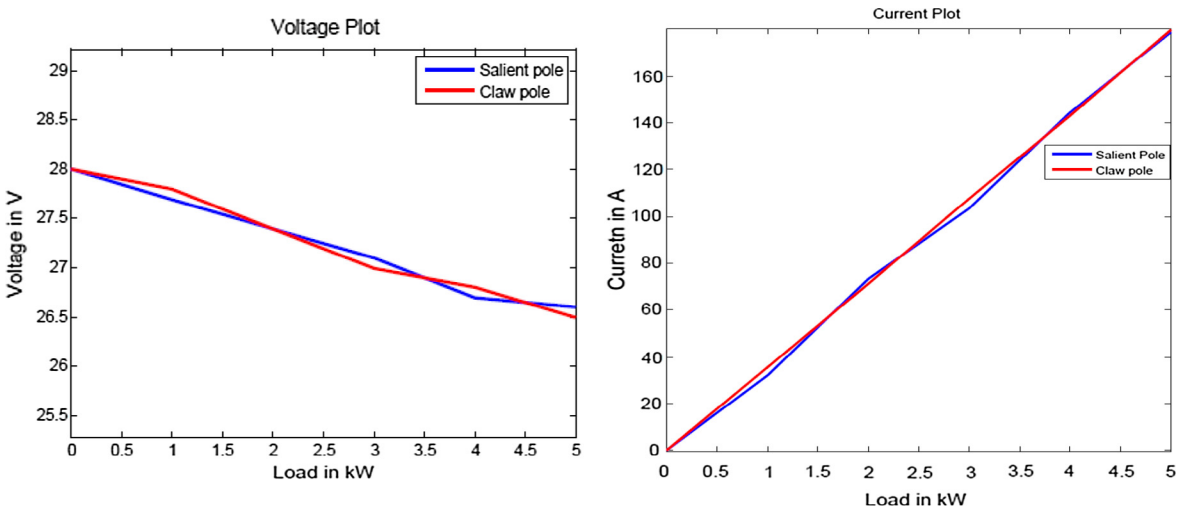

Figure 16 Load voltage and current.

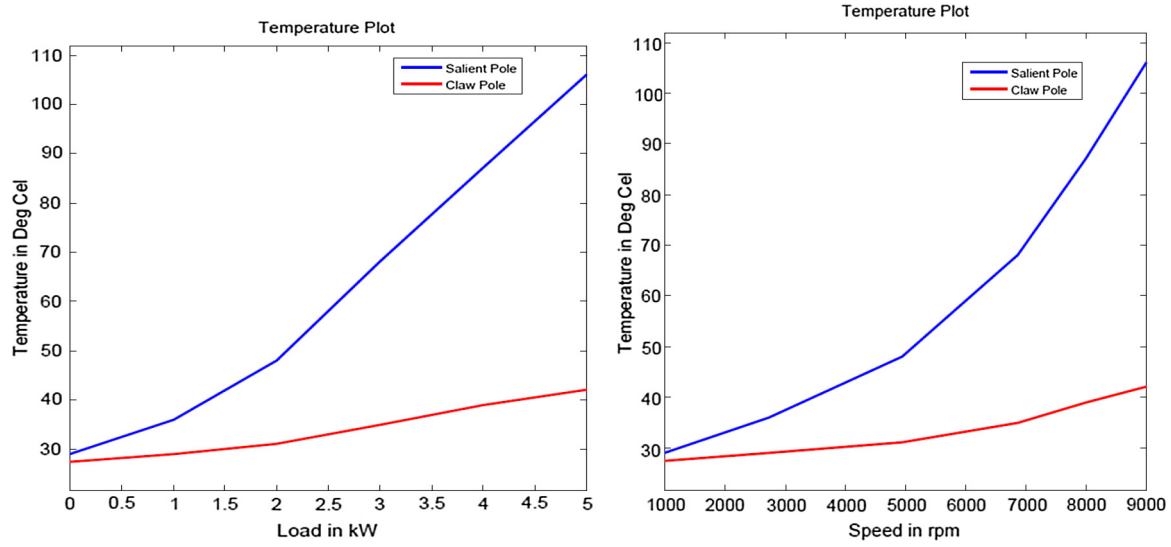

Figure 17 Temperature plot of CPA.

ratio of 1:6. Here both resistive load and lamp load are connected across the generator.

The prototype model of the 5 KW claw pole alternator was fabricated and tested in the laboratory. The snapshot of the alternator is shown in Fig. 15. It consisted of 5 KW claw pole alternator, induction motor acting as prime mover, gear box, generator control unit and load bank. The performance of the generator was tested under the speed of 2000–9000 rpm.

The output voltage and the current were measured using voltmeter and clamp meter. The voltage and the current waveforms from no-load to full load are shown in Fig. 16 for both generators and it is observed that the output voltage and the current are approximately equal to 28 V and 180 A respectively at full load condition during transient condition. The output voltage and the current could be maintained constant by using a Cuk converter with nonlinear controller.

The temperature of the SPA and CPA was measured using temperature indicator in stator core at the speed of 9000 rpm. This indicator connected in various parts of the generators measures the temperature at various load conditions. The temperature plot of SPA and CPA is shown in Fig. 17. The major problem in the temperature plot for SPA is that temperature reaches more than 90 °C within few minutes for loaded condition and rated speed condition. This problem occurs in SPA due to less airgap area and large current produced in small dimension. Similarly it was seen that for same duration the temperature of CPA was below 42 °C when the machine was operating at maximum speed and load conditions. That is claw pole rotor has large airgap compared to salient pole rotor.

The performance comparison between salient pole and claw pole is given in Table 3 based on results obtained from hardware testing. From the table it can be seen that both the voltage and the current ratings are approximately equal for both rotor structures. But the temperature value is high in salient pole alternator within short duration due to less airgap area and low air circulation inside the aircraft. On the other hand,

Table 3 Performance comparison between SPA and CPA.

Parameter	Salient pole	Claw pole
Power rating in KW	5	5
Voltage in V	27.8	27.5
Current in A	178.5	179.2
Temperature in °C	98.7	41.2

temperature generated inside the claw pole alternator is below 42 °C due to more airgap space when compared to salient pole rotor.

7. Conclusion

In this work the coupled electromagnetic and thermal analysis of the alternator having two different rotors for aircraft application was presented. The thermal based analytical modeling of an alternator was given. The simulation analysis of the 5 KW alternator for both rotors was carried out using FEA software. Similarly the prototype models of the 5 KW salient pole and claw pole alternators were tested in the laboratory. In simulation analysis both generators produced required power and less temperature during electromagnetic and thermal analysis. Also in the both generators the maximum temperature was produced at rotor conductors and stator core outer surface. During hardware testing, SPA generates more heat at full load and rated speed condition. The heat generation in CPA is not very high for both analyses due to large airgap and airflow. So, it was observed that the thermal performance of a claw pole alternator was better than the salient pole alternator during high speed operations. But the electromagnetic performance of both alternators was found to be suitable for high speed operations.

The performance of the claw pole alternator with permanent magnet rotor or stator will be studied in the future. The thermal performance of the claw pole alternator used in this study may be improved upon by adjusting the pole shape of the claw to get better ventilation and airflow.

References

[1] Ahmed Abdel-Hafez, Recent Advances in Aircraft Technology, In Tech Press, China, 2012.
[2] Aldo Boglietti, Andrea Cavagnino, David Staton, Martin Shanel, Markus Mueller, Carlos Mejuto, Evolution and modern approaches for thermal analysis of electrical machines, IEEE Trans. Ind. Electron. 56 (2009) 871–881.
[3] Carlos Mejuto, Abdeslam Mebarki, David Staton, Nazar Al-Khayat, Markus Mueller, Thermal modeling of TEFC alternators, in: 32nd Annual Conference of IEEE Industrial Electronics Society, Paris, 2006, pp. 4813–4818.
[4] Carlos Mejuto, Improved Lumped Parameter Thermal Modeling of Synchronous Generators, The University of Edinburgh, 2010.
[5] Cassandra Bailey, Daniel M. Saban, Dalvis Gonsalez-Lopez, Design and experimental evolution of high speed directly coupled multi megawatt permanent magnet synchronous generator, in: Proceedings of the 38th Turbo Machinery Symposium, 2009, pp. 137–148.
[6] Charanjiv Gupta, Sanjay Marwaha, Manpreetsingh Manna, Finite element is an aid to machine design: a computational tool, in: COMSOL Conference, 2009, pp. 1–6.
[7] David Staton, Stephen Pickering, Desmond Lampard, Recent Advancement in the Thermal Design of Electric Motors, Emerging Technologies for Electric Motion Industry, Durham, North Carolina, USA, 2001.
[8] Deepak Arumugam, Premalatha Logamani, Performance evaluation of brushless exciter for aircraft applications, Aust. J. Basic Appl. Sci. 8 (2015) 151–158.
[9] Deepak Arumugam, Premalatha Logamani, Coupled magnetic field and thermal analysis of synchronous generator, Aust. J. Basic Appl. Sci. 8 (2014) 124–131.
[10] M. Feistauer, Finite Volume and Finite Element Methods in CFD (Numerical Simulation of Compressible Flow), Charles University, Prague, 2007.
[11] F. Gieras, New applications of synchronous generators, Przeglad Elektrotechniczny (2015) 151–157.
[12] http://www.tejas.gov.in/.
[13] Huijuan Liu, Longya Xu, Mingzhu Shangguan, W.N. Fu, Finite element analysis of 1 MW high speed wound-rotor synchronous machine, IEEE Trans. Magn. 48 (2012) 4650–4653.
[14] Ivan Jadric, Dusan Borojevic, Martin Jadric, Modeling and control of a synchronous generator with an active DC load, IEEE Trans. Power Electron. 15 (2000) 1–8.
[15] T. Lange, F. Qi, J. Dehn, R.W. De Doncker, Synchronous machine model considering dynamic losses and thermal behavior, in: IEEE International Electric Machines & Drives Conference, 2015, pp. 536–542.
[16] A. Lebsir, R. Rebbah, M. Larakeb, H. Djeghloud, A. Bentounsi, Modeling and analysis of a salient poles synchronous machines using finite-elements method, in: International Symposium on Power Electronics, Electrical Drives, Automation and Motion, 2014, pp. 363–367.
[17] Lucian Tutelea, Dragos Ursu, Ion Boldea, Sorin Agarlita, IPM claw-pole alternator system for more vehicle braking energy recuperation, J. Electric. Eng. (2008) 1–10.
[18] Martin Stöck, Quentin Lohmeyer, Mirko Meboldt, Increasing the power density of e-motors by innovative winding design, in: CIRP 25th Design Conference Innovative Product Creation, 2015, pp. 236–241.
[19] Plejic, Matjaz Gorican, Viktor Hribernik, Bozidar, FEM thermal modeling of an induction motor, in: André Nicolet, R. Belmans (Eds.), Electric and Magnetic Fields, Springer, US, 1995, pp. 155–158.
[20] St. Schulte, K. Hameyer, Multi-physics simulation of a synchronous claw-pole alternator for automotive applications, IEEE Trans. Magn. (2005) 896–901.
[21] W.L. Soong, Thermal Analysis of Electrical Machines: Lumped-Circuit, FE Analysis and Testing, Power Engineering Briefing Note Series, 2008, pp. 21–22.
[22] D.A. Staton, S. Pickering, D. Lampard, Recent advancement in the thermal design of electric motors, in: SMMA Technical Conference – Emerging Technologies for Electric Motion Industry, 2001, pp. 1–7.
[23] D.A. Staton, Boglietti, A. Cavagnino, Solving the more difficult aspects of electric motor thermal analysis, in: IEEEIEMDC 2003 Conference Proc, 2003, pp. 1–4.
[24] Z. Xu, A.L. Rocca, S.J. Pickering, C. Eastwick, C. Gerada, S. Bozhko, Mechanical and thermal design of an aero engine starter/generator, in: IEEE International Electric Machines & Drives Conference, 2015, pp. 1607–1613.
[25] Zimin W. Vilar, Dean Patterson, Roger A. Dougal, Thermal analysis of a single sided axial flux permanent magnet motor, in: 31st Annual Conference of IEEE Industrial Electronics Society, Paris, 2005.
[26] Zlatko Kolondzovski, Thermal and Mechanical Analyses of High-Speed Permanent-Magnet Electrical Machines, Aalto University, 2010.

Please cite this article in press as: D. Arumugam et al., Electromagnetic & thermal analysis of synchronous generator with different rotor structures for aircraft application, Alexandria Eng. J. (2017), http://dx.doi.org/10.1016/j.aej.2017.03.020